PHILOSOPHICAL TRANSACTIONS A

rsta.royalsocietypublishing.org

Research

Cite this article: Bonechi L *et al*. 2019 Tests of a novel imaging algorithm to localize hidden objects or cavities with muon radiography. *Phil. Trans. R. Soc. A* **377**: 20180063. http://dx.doi.org/10.1098/rsta.2018.0063

Accepted: 19 October 2018

One contribution of 21 to a Theo Murphy meeting issue 'Cosmic-ray muography'.

Subject Areas:
high-energy physics, particle physics, geophysics

Keywords:
muon, radiography, imaging

Author for correspondence:
L. Bonechi
e-mail: Lorenzo.Bonechi@fi.infn.it

Tests of a novel imaging algorithm to localize hidden objects or cavities with muon radiography

L. Bonechi[1,2], G. Baccani[1,2], M. Bongi[1,2], D. Brocchini[3], N. Casagli[4], R. Ciaranfi[1], L. Cimmino[5,6], V. Ciulli[1,2], R. D'Alessandro[1,2], C. Del Ventisette[4], A. Dini[7], G. Gigli[4], S. Gonzi[1,2], S. Guideri[3], L. Lombardi[4], B. Melon[1], N. Mori[1,2], M. Nocentini[4], P. Noli[5,6], G. Saracino[5,6] and L. Viliani[1]

[1]INFN Firenze, Via B. Rossi 3, 50019 Sesto F.no (Firenze), Italy
[2]Università di Firenze, Dipartimento di Fisica e Astronomia, Via G. Sansone 1, 50019 Sesto F.no (Firenze), Italy
[3]Parchi Val di Cornia, Via Giovanni Lerario 90, 57025 Piombino (LI), Italy
[4]Università di Firenze, Dipartimento di Scienze della Terra, Via La Pira 4, 50121 Firenze, Italy
[5]Università di Napoli Federico II, Dipartimento di Fisica, Via Cinthia 21, 80126 Napoli, Italy
[6]INFN Napoli, Via Cinthia 21, 80126 Napoli, Italy
[7]IGG-CNR, Via G. Moruzzi 1, 56124 Pisa, Italy

LB, 0000-0001-6097-1181; LC, 0000-0002-8888-8029; RD, 0000-0001-7997-0306

A novel algorithm developed within muon radiography to localize objects or cavities hidden inside large material volumes was recently proposed by some of the authors (Bonechi *et al*. 2015 *J. Instrum.* **10**, P02003 (doi:10.1088/1748-0221/10/02/P02003)). The algorithm, based on muon back projection, helps to estimate the three-dimensional position and the transverse extension of detected objects without the need for measurements from different points of view, which would be required

THE ROYAL SOCIETY PUBLISHING

to make a triangulation. This algorithm can now be tested owing to the availability of real data collected both in laboratory tests and from real-world measurements. The methodology and some test results are presented in this paper.

This article is part of the Theo Murphy meeting issue 'Cosmic-ray muography'.

1. Introduction

Currently, muon radiography is probably the only non-invasive technique that can be successfully exploited to measure the three-dimensional density profile of large volumes of material, such as portions of mountains or hills from tens to hundreds of metres deep, with a spatial/angular resolution that enables cavities or dense bodies with a linear size of the order of metres to be identified. The two different ways of exploiting the muon projectiles crossing a target volume, multiple scattering muon tomography (MSMT) and muon transmission radiography (MTR), are suitable for investigating volumes of different size. MSMT is usually exploited for relatively small objects, of the order of a few cubic metres at maximum, and provides three-dimensional information on the observed volume. It is in fact based on the multiple scattering effect, which was studied by means of two independent detectors located upstream and downstream of the target volume. The incoming and outgoing muon tracks are reconstructed for a large set of muons and exploited to determine the most likely density distribution inside the target volume, using custom iterative algorithms developed by the few research groups worldwide that are able to apply this technique and that have developed their own (not open source) code. Different from MSMT, MTR is a two-dimensional technique. It is based on a single muon telescope that is used to compare the muon flux downstream of a target volume with the flux measured in the absence of any target, the so-called free sky (FS) flux. The information that usually comes from such a measurement is a two-dimensional angular density profile of the target volume, i.e. an estimate of the average density of matter encountered along a direction within the field of view of the instrument. In many cases (e.g. [1,2]) with single muon radiography using the latter technique it is possible to identify 'anomalies' in muon transmission that could potentially be linked to unexpected cavities or dense objects located somewhere along the identified directions and subtending a measurable angular aperture with respect to the detector's position. No information is available at first glance on the linear size or the distance from the detector of the structures producing these anomalies in the angular density map. However, under quite general conditions it can be shown that this information can be obtained by exploiting the three-dimensional reconstruction of the muon tracks. The proposed method, the so-called back-projection method, supported by the results of simulations performed using the GEANT4 software [3], is illustrated in §2, and tests with real data are discussed in §3.

2. The back-projection method

The imaging method discussed in this paper and that is currently under test, designed within the context of MTR, is described in detail in [4]. Basically, it exploits the spatial extension of the detector to localize structures of interest hidden inside large material volumes. The requirements that the case study must satisfy for this method to hold its validity are basically geometric constraints. A detector deployed at some depth below the level of an object, with the object in its field of view, has in general a stereoscopic view of the object itself, in exactly the same way as our eyes have a stereoscopic view of any object placed in our field of view. Different parts of the detector in fact see an object along different directions and this remains valid until the distance of the object from the detector is not excessive with respect to the size of the detector itself. Otherwise, the detector could be approximated as a point-like detector, as is reasonable to do in the case of measurements of volcanic edifices, where small detectors, compared with the typical size of volcanoes, are located one or a few kilometres away from the target. If this

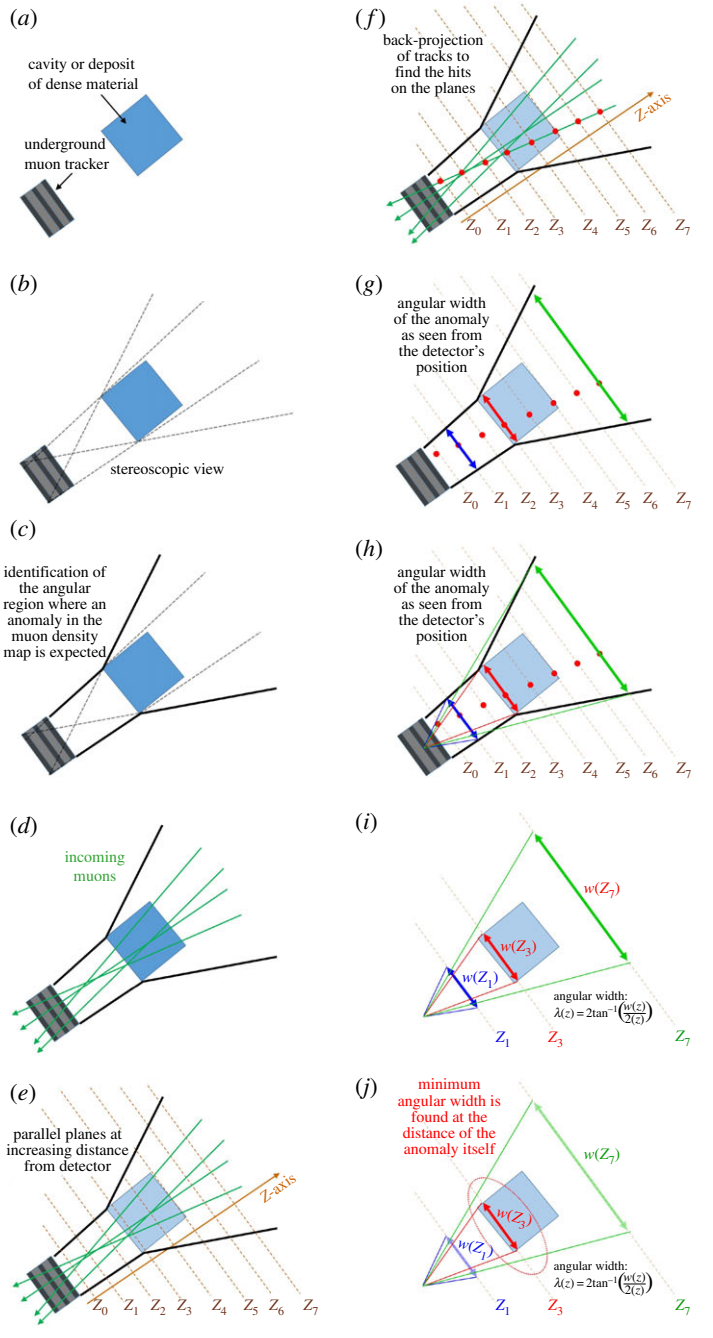

Figure 1. Main steps of the back-projection method. Details can be found in the text (§2).

geometrical constraint holds, then it would be possible to perform a sort of internal triangulation of data, exploiting the muon transmission maps obtained for each part of the detector separately. This is what is implemented in the back-projection method.

Figure 1 illustrates the main points that can be used to explain this simple method.

First of all, we assume that we have a muon tracker deployed inside some wide material volume and an object (cavity or metal deposit) positioned not very far from it, in its field of view (figure 1*a*). In the example, the object has been drawn just in front of the detector and very close to it, while in a realistic case a more complicated geometry should be considered. The method can

be generally applied, if we assume that the distance of the object from the detector is not very large with respect to the size of the instrument. In this case, each point of the target is seen from the detector under different angles (figure 1*b*), allowing a sort of stereoscopic vision of the object. Lines going from the centre of the detector to the most external points of the object are shown. In this extremely simplified two-dimensional representation, the range of incoming angles within the detector's acceptance at which we can expect to find a signal in the muon transmission map due to the presence of the object (figure 1*c*), also ignoring the multiple Coulomb scattering effect, is determined by muons whose tracks run completely within the limits defined by these lines. After the reconstruction of a whole set of muon tracks (figure 1*d*) collected in the same geometrical configuration we expect thus an 'anomalous' number of events in this angular region. The definition of custom surfaces at different distances from the detector allows the study of how this angular region develops in space. A possible choice of these surfaces could be a bundle of parallel planes, orthogonal to the detector's axis, as shown in figure 1*e*, but different choices could be appropriate depending on the case study, such as a bundle of concentric spheres and horizontal or vertical planes. All the reconstructed tracks, including the whole detector's acceptance, can then be backwards propagated as straight lines and projected onto each of these surfaces (figure 1*f*) in such a way as to determine the hit point distribution on each of them. We thus expect an 'anomalous' density of hit points in a region representing the projection of the shape of the object on the surfaces along the directions allowed by the detector's acceptance (figure 1*g*). The angular width subtended by these regions with respect to the detector's centre depends clearly on the position of the back-projection plane, as shown by the coloured lines drawn in figure 1*h*. On the basis of purely geometrical considerations, it is possible to see that the size of the angular width just defined decreases going from the detector to the object location and then increases slowly at higher distances (figure 1*i*), remaining near the minimum value along the extension of the object. The minimum angular width is thus reached when the back-projection surface approaches the object.

This geometrical property can then be exploited to give an estimate of the distance from the detector of an object producing a signal in the muon transmission map. When considering the back-projection to a plane at the distance where the minimum of the angular width is found, the linear extension of the 'anomalous' region gives information on the linear extension of the hidden object.

In this way, using single muon radiography performed with a single muon tracking system, we can obtain three-dimensional information that is useful for the characterization of an unknown object located in the field of view of the instrument. This information can also be used to define a new detector's installation point to provide a second measurement, which can be optimized to allow for triangulation of the detected object.

3. First tests with real data

The back-projection method described in §2 is currently being tested for the first time using real datasets collected both with test measurements performed in our laboratories and with on-field measurements in cases of archaeological or geological interest. In §3a,b, we present the preliminary results of two of these tests, which give an indication of the potential uses of this method.

(a) Detection of metal blocks in the laboratory

The first test with real data using the back-projection method dates back to the first half of 2017. The purpose of this test was to identify the muon absorption effect due to the presence of metal blocks in front of a hodoscope. For this measurement, a tracking system based on five double-sided silicon microstrip detectors taken from the ADAMO magnetic spectrometer [5] was used. Each silicon sensor, 300 µm thick, had an area of $5.33 \times 7.00\,\mathrm{cm}^2$ and was held inside a light-tight aluminium frame. Three sensors were stacked horizontally very close to one another (8 mm) in

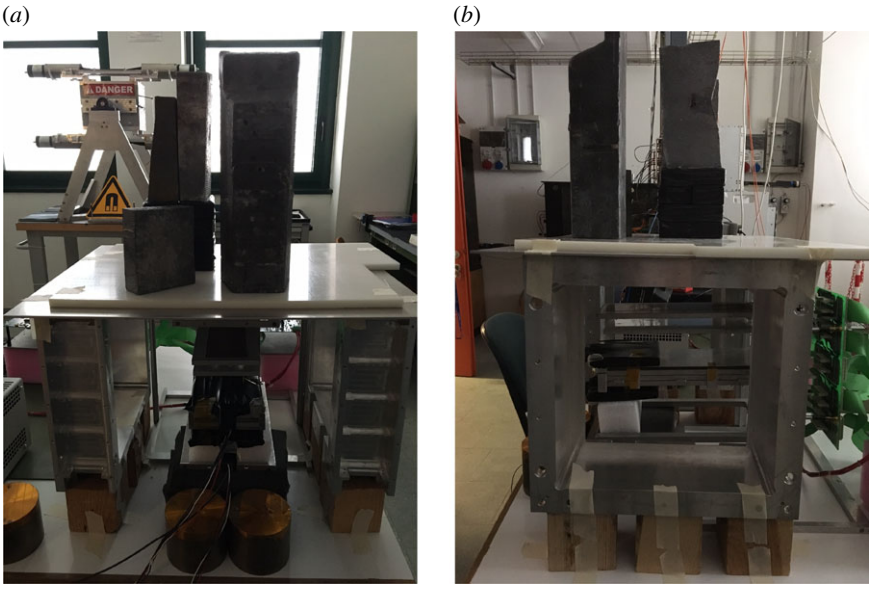

Figure 2. The set-up used for a laboratory test of the back-projection method. (*a*) Front view. (*b*) Right-side view. Three lead assemblies were positioned on a horizontal plane and held in place by two strong vertical aluminium frames. The system used for muon tracking, made of five double-sided silicon microstrip planes, is visible in the region below the plane. In the background of (*a*), on the left side, the magnetic system of the ADAMO magnetic spectrometer, from which the tracking system was extracted for this test, can be clearly identified. (Online version in colour.)

such a way as to maximize the geometrical acceptance, given the small linear size of the sensors. Two additional sensors were positioned above this triplet, a few centimetres away, and were not used for event selection. Even with this trick the resulting total geometrical factor is of the order of 70 cm^2 sr, which is quite small for this kind of application, where a large number of events are required to discover the suppression effects of the order of a few per cent on the FS muon flux. Moreover, the silicon planes used for this measurement have quite a low efficiency, due mainly to many defects in the implantations and a few malfunctioning chips on the front-end electronics.

The test was divided into two different and independent measurements. At first, data were acquired with metal blocks placed in the field of view of the detector. The set-up is shown in figure 2. Three separate metal assemblies, made of lead tiles and blocks, were positioned on a horizontal plane held above the tracking system by two aluminium structures. The distance between the lowest silicon sensor and this plane was approximately 22 cm. In this 'target' configuration, 616 114 events were collected in approximately one week.

After the first phase, the lead blocks were removed from the tracker's acceptance, leaving all the other structures in place, and an FS measurement of muon flux was obtained for comparison with the previous measurement. In this different configuration, 634 915 events were collected in approximately one week. The overall difference between the two measurements was approximately 3%, but on looking at the data this has to be restricted to the angular regions subtended by the lead blocks.

Figure 3 shows the measured angular muon transmission map, i.e. the ratio between the target and the FS measurements, after correcting for the slightly different duration of the two data acquisitions. The direction of motion of the muons, i.e. the angles defined by their trajectories, is determined after track identification and fitting. Only the angular information is used to build the muon transmission map, while the information on the hit point on the detector is ignored. The results are reported in a pseudo-polar reference frame where the centre of the plot corresponds to the vertical direction, the distance of a bin from the centre corresponds to the polar angle and

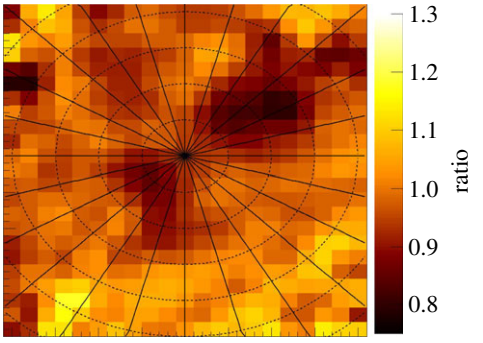

Figure 3. Measured angular distribution of muon transmission for the laboratory test measurement of the back-projection method. (Online version in colour.)

the rotation around the centre corresponds to the azimuth angle. The polar grid shown in this plot (and in the following plots using the same reference system) has 10° and 15° steps for the polar and azimuth angles, respectively. Despite the short time required to gather the data, the shadows of the lead blocks can be identified in the muon transmission histogram. However, each point in the space is seen by the tracker under quite different angles, given the geometry chosen for this test; therefore, the signal coming from the boundaries of the metal blocks is noisy and the resulting image is not very well defined.

A better imaging result is obtained using the back-projection method, which exploits not only the angular information about the muon trajectories but also their hit points. The complete three-dimensional reconstructed tracks are backwards projected and intersected with parallel planes orthogonal to the detector's line of sight. Two-dimensional histograms of the difference in the counts obtained in the T and FS measurements are built for each of these planes. It is clear that this type of representation does not give the same weight to all the bins, owing to the different acceptance values of the detector at different angles and the dependence of the muon flux on the zenith angle. Nonetheless, after we identified a not-too-extended signal and focused only on that, these histograms could be used safely for measuring its angular size, as is required in the back-projection method. The results of the analysis are shown in figure 4.

Figure 4*a–i* shows the two-dimensional 'difference' histograms built for the back-projection planes with Z, representing the distance from the detector's external surface, between 0 cm and 40 cm. The bin size of these histograms increases linearly with Z in such a way as to conserve the equivalence between the number of bins and the angle subtended with respect to the centre of the detector. If no target was placed in front of the detector, we would expect the content of each bin to be dominated only by statistical fluctuations. The plot at $Z = 0$ shows all the hit points confined on a 5.33×7.00 cm surface, corresponding to the size of a silicon sensor. No clear image of the metal structures can be identified, but it is straightforward to observe that most of the bins report negative counting, owing to the presence of the lead blocks in front of the tracker. For larger Z the surface covered by hit points increases in size and at $Z > 10{-}15$ cm three signal structures become clear. The histogram shown in figure 4*f* has been chosen for a test of the back-projection method. The purpose of this test was to try to estimate the distance of the corresponding lead block from the tracker. The angular width of the signal was evaluated in a simple way by making projections of bin values in the signal region of these histograms to the horizontal axis and making a Gaussian fit of the 1-dim signal peak. Figure 4*j* shows the dependence of the angular size of the selected signal on the Z-coordinate. A minimum angular size is found for $Z \simeq 20$ cm, which corresponds approximately to the distance of the object from the detector.

Figure 5*a* shows as an example a comparison between the back-projected 'difference' histogram on the plane at $Z = 35$ cm. A global agreement with the known size and position of the lead blocks is found. Figure 5*b* shows the metal structures.

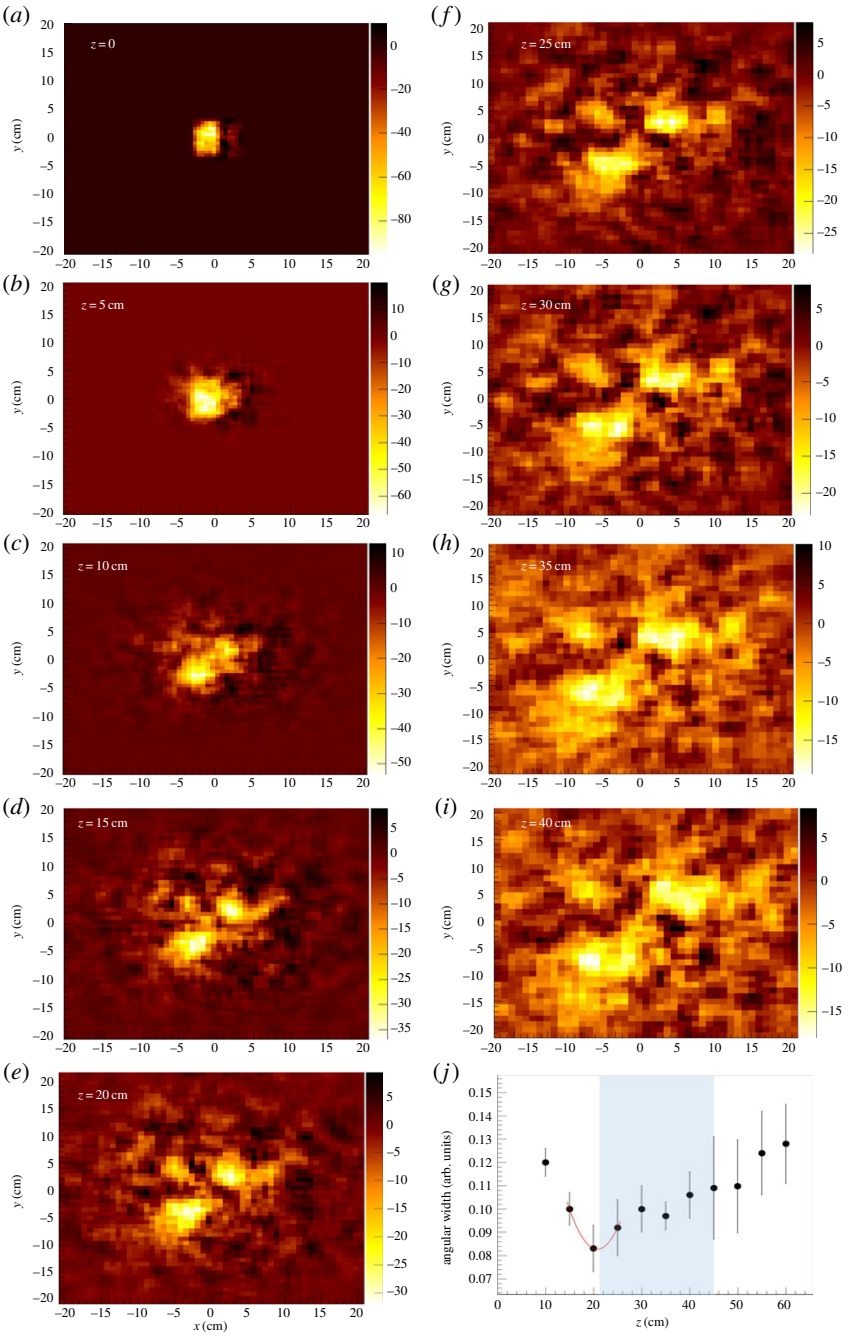

Figure 4. (*a–i*) T–FS histograms obtained after back-projecting tracks to planes at different distances from the detector. (*j*) The dependence on the *Z*-coordinate of the function describing the angular size of an identified signal region. The shaded area is the region covered by the selected lead block. The minimum of the function is found in correspondence to its nearest face. (Online version in colour.)

(b) Preliminary results at the Temperino Mine

The same data analysis technique previously described and applied to the test discussed in §3a can also be applied in principle to cases where larger volumes are involved. Using data collected

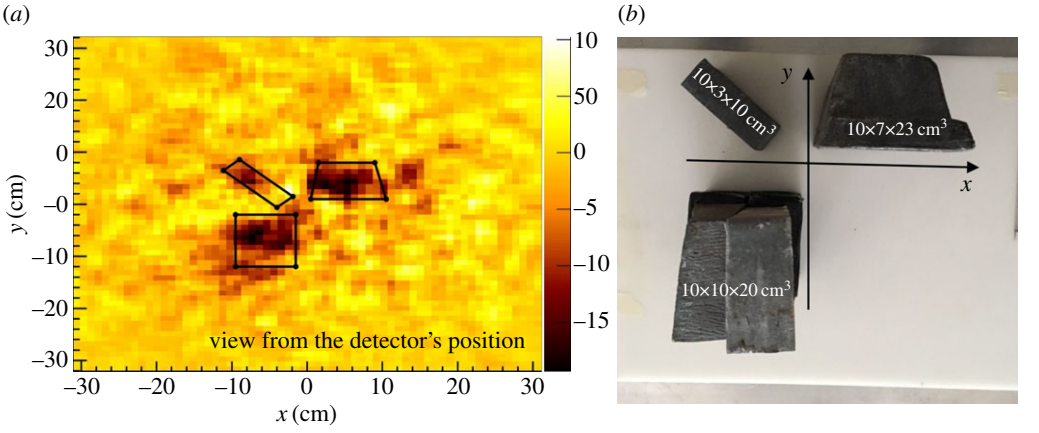

Figure 5. (*a*) Comparison of signals appearing in the difference map obtained after back-projecting muon tracks to a plane 35 cm far from detector with the known geometrical shapes of the lead blocks. (*b*) Photo of the lead blocks during the measurement. (Online version in colour.)

inside an old mine not far from Florence, Italy, by means of the muon imaging for mining and archaeology (MIMA) detector [6], we have tried to determine the distance from the detector of known empty volumes visible on the muon transmission map. Details of the data analysis were presented at the 7th International Conference on New Frontiers in Physics, which was held in Crete, Greece, during July 2018 (https://www.mdpi.com/journal/universe).

Data used in this preliminary study were collected between the end of 2017 and the beginning of 2018. The MIMA detector, a muon tracker with a geometrical factor of 1000 cm^2 sr with an angular resolution of approximately 10 mrad, was installed inside a tunnel, in a position approximately 30–40 m below the collapse of a surface quarry, which is visible on the surface. The measurement direction was aligned along the vertical direction, pointing directly at the collapse point, to test the detector's capability of identifying the known cavities and galleries and hopefully finding some unknown structures. The total acquisition time for this measurement was 53.5 days and the measured trigger was around 0.5 Hz, for a total of more than 2.3 million events saved to disk. The FS measurement along the vertical direction, which was necessary for a comparison to produce the muon transmission map, was carried out after the measurement in the gallery. To simplify the logistics this measurement was performed in the areas outside the INFN building in Sesto Fiorentino (Florence, Italy), given the negligible variation expected between the two locations. The detector was exposed for 17.3 days and measured a trigger rate of around 22 Hz, finally collecting more than 35 million events.

In figure 6, the angular distributions of muon tracks collected in the FS and T measurements are shown in the polar angular reference frame described in the previous section. The differences between the two measurements can be clearly seen. The angular distribution of tracks in the FS measurement has a symmetric shape around the zenith (centre of the plot); the non-circular underlying shape is due to the square shape of the detector's tracking planes, which show a larger acceptance along the two preferential directions.

Figure 7 shows the two-dimensional angular distribution of the muon transmission, i.e. the fraction of muons that are able to reach the detector. Figure 7*a* shows the ratio between the T and FS measurements, after normalizing for the different durations of the data acquisitions. The blue regions, i.e. those for which muon transmission is more suppressed, can be explained as being due to the rising of the overlying hill's surface towards the northeast. The dependence of muon transmission on the shape of the hill has not been subtracted from this plot. To remove this effect, muon transmission has been simulated using a digital elevation model of the area around the mine and the knowledge of the detector's installation position. In figure 7*b* the simulated

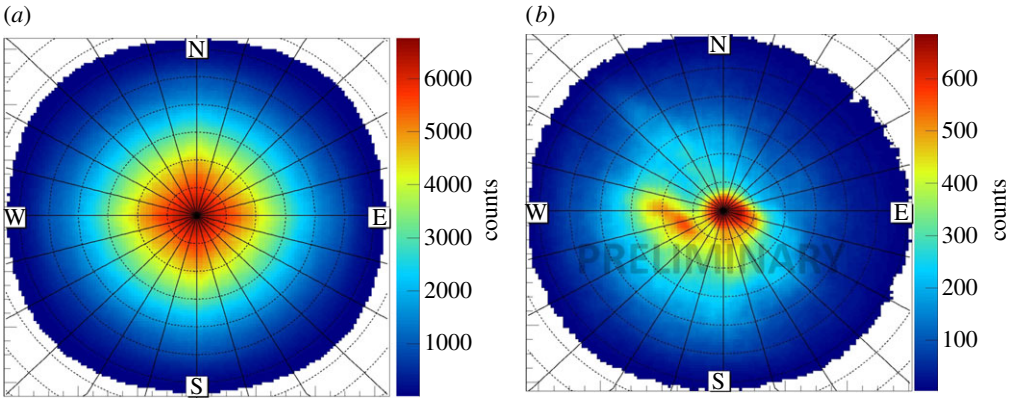

Figure 6. Angular distributions of incoming muon tracks measured along the vertical direction at FS (*a*) and inside the Temperino mine (*b*).

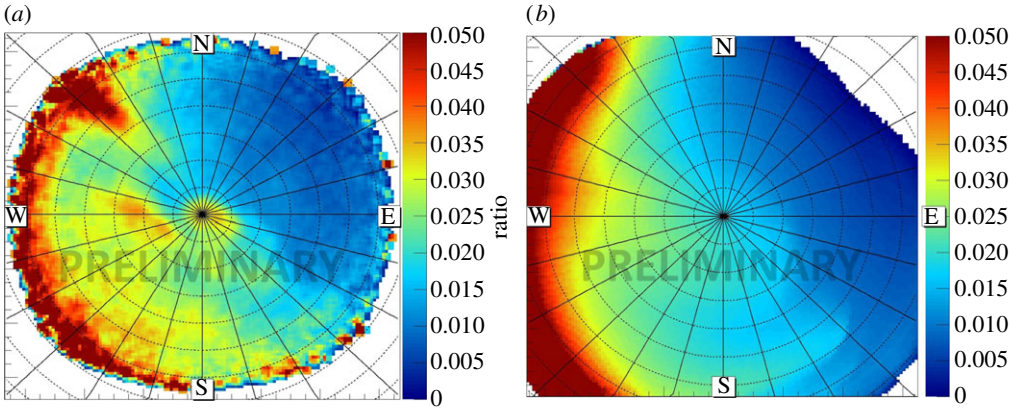

Figure 7. Measured (*a*) and simulated (*b*) angular distribution of muon transmission.

muon transmission expected in the case of uniform rock with an average density of 3.0 g cm^{-3} is shown. Comparing this plot with the measured transmission a general agreement is found, but many 'anomalies' in the measured distribution can be clearly identified that are not found in the simulation.

A comparison of the measured muon transmission map with maps simulated using different rock densities allows the two-dimensional angular density map to be reconstructed; this is shown in figure 8*a*. In this plot some angular regions with an average density that is lower than expected can be identified. Some of these regions correspond to the angular regions covered by known cavities. The already mentioned terrain collapse is visible along the vertical direction (low-density angular region at the centre of the plot).

The anomalous zone developing in the northwest direction corresponds to a large empty volume of Etruscan age called 'Gran Cava' (figure 9), which is easily accessible nowadays from the surface of the hill. The other anomalies found by the muon radiography described here are still under study with the help of geologists and speleologists and may correspond to ancient excavations reported on some maps, but that are no longer accessible.

The first region chosen for testing the back-projection method is the region of the Gran Cava. Owing to the intense signal in the transmission map due to its geometric extension and the possibility to easily access it, this region allows a better check of the results than other regions.

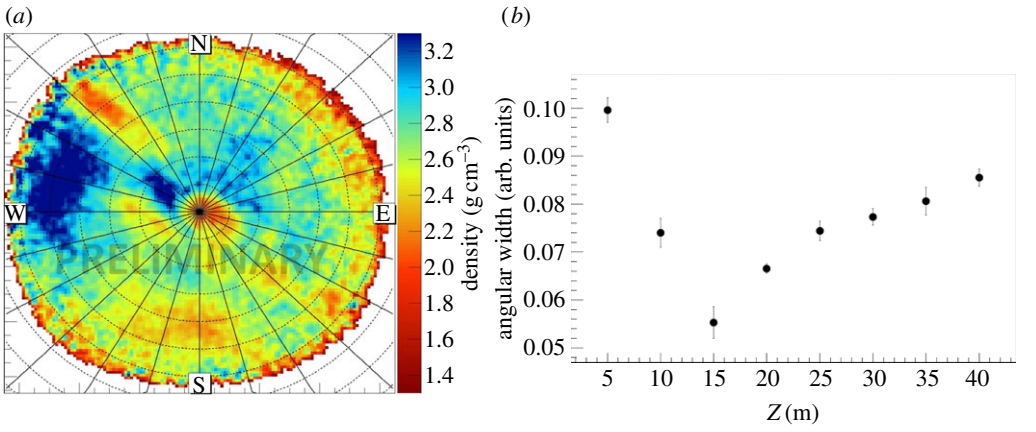

Figure 8. (*a*) Two-dimensional angular density map measured along the vertical direction at the Temperino mine. (*b*) Result of the back-projection method applied to the measurements at the Temperino mine, showing the dependence of the angular width subtended by the region containing the signal due to a known cave (the Gran Cava) on the distance of the back-projection plane from the detector. A minimum is found for Z between 15 m and 20 m. This is not very different from the value obtained on the basis of a three-dimensional laser scanner survey, which showed that the altitude difference between the detector and the base of the Gran Cava is (21 ± 2) m.

Figure 9. The so-called Gran Cava above the Temperino mine. The measured width is around 4—6 m and the height around 6—7 m depending on the position. (Online version in colour.)

T–FS histograms have been produced for horizontal back-projection planes up to $Z = 40$ m (maximum distance from the detector's upper surface). The same algorithm presented in the previous section has been used to evaluate the dependence on the Z coordinate (i.e. the distance from the detector) of the angular width subtended by the region containing the signal. The result is reported in figure 8*b*. This plot shows a trend that is very similar to the expected trend based

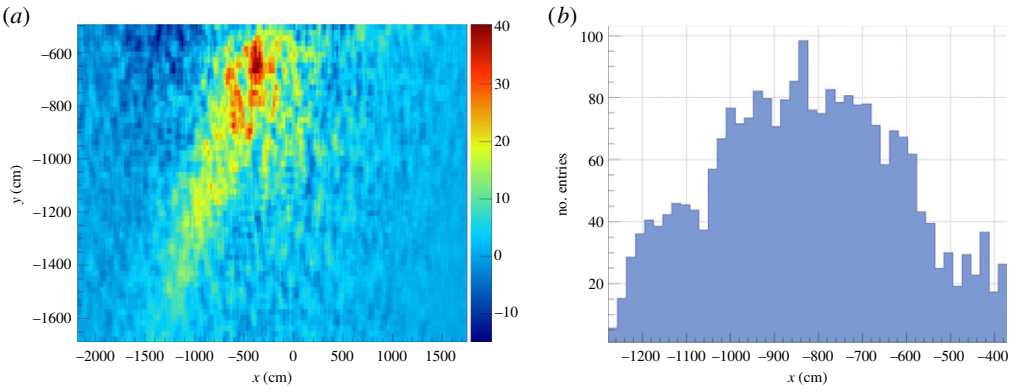

Figure 10. (*a*) Signal produced by the 'Gran Cava' in the back-projection difference map at 16 m from MIMA. (*b*) Projection to the *X*-axis of the content of a few bins in the region around $y = -10$ m.

on very simplified geometrical assumptions, as discussed in [4]. A minimum of the function describing the angular width subtended by the identified signal is found on a back-projection plane located at an altitude between 15 m and 20 m higher than that of the position where the detector was installed. The difference in altitude between the detector's location and the base of the Gran Cava is known owing to an accurate geometrical survey that we have obtained using a three-dimensional laser scanner. As will be shown elsewhere we now have a three-dimensional scan of the relevant part of the surface of the hill and of the interior of the Temperino mine and of the Gran Cava. Based on this survey, the altitude difference between the detector and the base of the Gran Cava was found to be (21 ± 2) m (the large uncertainty takes into account the uneven ground inside the Gran Cava). This value is slightly larger than the value found with the back-projection method. This result requires careful verification and could be linked to the fact that we do not know the exact structure of the material contained between the position of the detector and the Gran Cava. In fact, we have already identified some tunnels near the detector's location that cannot be easily accessed due to the collapse of material from above. The observed effect could then be due to some cavities still present below the Gran Cava floor. Apart from these comments, which could be important for the optimization phase of the technique, the result is positive for the test of the methodology, which seems to also work in the case of very large volumes and bodies with respect to the case presented in §3a. Looking finally at the back-projection difference map on a plane 16 m far (higher) than the detector, we find the image shown in figure 10*a*.

The image is seen from the point of view of the underground detector and it appears to be mirrored with respect to the transmission maps shown before, where it is viewed from above in order to compare it with geographical maps. The signal due to the empty volume of the Gran Cava is clear. Figure 10 shows a projection to the *X*-axis of the content of five bins in the region around $y = -10$ m. Most of the signal develops for $-10.5\,\text{m} < x < -5.5\,\text{m}$, suggesting a width of approximately 4 m, in quite good agreement with the measured size.

4. Conclusion

The work reported in this paper describes some tests of a new methodology recently developed by some of the authors within MTR. This methodology is based on a muon track back-projection technique that allows the distance and size of cavities or dense objects eventually localized by means of muon radiography performed from a single detector's installation point to be estimated. This technique could be used to provide initial three-dimensional information on the structures previously identified within the detector's field of view. The reconstruction of a real

three-dimensional density map of the analysed volume is however much more complicated and requires measurements from multiple points of view.

From the results of recent tests, carried out both in the laboratory for metal detection and inside the Temperino mine in Tuscany (Italy) for the identification of large cavities, we had the first indications about the performance of the proposed methodology. The results of some of these tests have been presented in this work. More careful tests will be performed by exploiting ongoing measurements that we are carrying out in different fields of application. These tests will help to confirm the validity of this methodology.

Data accessibility. This article has no additional data.

Authors' contributions. L.B., R.D., L.V. and N.M. are the main developers of the back-projection method described in this article. L.B. and G.B. carried out the data analysis. S.G., M.B., N.M., L.V. and V.C. were involved in the development of the simulation software. Concerning the hodoscope used at the Temperino mine, L.B., R.D., G.B., B.M. and R.C. were the main developers and G.S., P.N. and L.C. provided the readout electronics. C.D.V., G.G., L.L., M.N. and N.C. carried out the 3D geometrical survey for the measurement at the Temperino mine. S.G. and D.B. were the main reference for the activity at the Temperino mine. S.G., A.D. and D.B. were the main consultants for the archaeological and geological matters at the site of the Temperino mine. All authors read and approved the manuscript

Competing interests. The authors declare that they have no competing interests.

Funding. We gratefully acknowledge funding from Istituto Nazionale di Fisica Nucleare (INFN) and the University of Florence.

References

1. Saracino G *et al.* 2017 Imaging of underground cavities with cosmic-ray muons from observations at Mt. Echia (Naples). *Sci. Rep.* **7**, 1181. (doi:10.1038/s41598-017-01277-3)
2. Morishima K *et al.* 2017 Discovery of a big void in Khufu's Pyramid by observation of cosmic-ray muons. *Nature* **552**, 386–390. (doi:10.1038/nature24647)
3. Viliani L. 2013 Muon radiography of underground structures using a hodoscope: feasibility study and first developments. Masters thesis, Università degli Studi di Firenze, Florence, Italy.
4. Bonechi L, D'Alessandro R, Mori N, Viliani L. 2015 A projective reconstruction method of underground or hidden structures using atmospheric muon absorption data. *J. Instrum.* **10**, P02003. (doi:10.1088/1748-0221/10/02/P02003)
5. Bonechi L, Bongi M, Fedele D, Grandi M, Ricciarini S, Vannuccini E. 2005 Development of the ADAMO detector: test with cosmic rays at different zenith angles. In *Proc. of the 29th Int. Cosmic Ray Conf. (ICRC 2005), Pune, India, 3–11 August 2005*, vol. 9, pp. 283–286. Mumbai, India: Tata Institute of Fundamental Research.
6. Baccani G *et al.* 2018 The MIMA project. Design, construction and performances of a compact hodoscope for muon radiography applications in the context of archaeology and geophysical prospections. *J. Instrum.* **13**, P11001. (doi:10.1088/1748-0221/13/11/P11001)